The spectroscopic search for water in barite group sulfates

Laurence Hopkinson[a*], Petra Kristova[b] Ken J. Rutt[b]

[a](*corresponding author)

[a] School of the Environment and Technology,

University of Brighton

Cockcroft Building, Lewes Road, Brighton. BN2 4GJ.

United Kingdom.

Tel: +44 (0)1273 642239, Fax: +44 (0)1273 642285, e.mail: l.hopkinson@brighton.ac.uk

[b] School of Pharmacy and Biomolecular Sciences,

University of Brighton.

Huxley Building, Lewes Road, Brighton.BN2 4GJ.

United Kingdom.

Tel: +44 (0)1273 642065, Fax: +44 (0)1273 642285, e.mail: p.kristova@brighton.ac.uk

Tel: +44 (0)1273 642076, Fax: +44 (0)1273 642285, e.mail: k.j.rutt@brighton.ac.uk

Key words: sulfates, near-infrared, mid-infrared, lead, strontium, barium.

Abstract

This study examines the mid and near infrared spectra of a suite of natural and synthetic powdered minerals of the isostructural barite mineral group. The mid-infrared (MIR) spectra are wholly compliant with anhydrous high purity anglesite, celestine and barite. The complementary near-infrared (NIR) spectra contain bands at *ca* 1.9μm (5263cm^{-1}) and *ca* 1.4μm (7140 cm^{-1}) assigned to the (H_2O) v_2 (antisymmetric stretch) + v_3 (bending vibration) combination band and overtones of the fundamental OH stretching modes respectively. Peak-fitting of the ca 4660-6000cm^{-1} region of interest reveals four shoulders to the (H_2O) (v_2 + v_3) combination which are systematically ordered with respect to interstitial metal covalent radius: [$PbSO_4$] (lowest wave number) → [$SrSO_4$] → [$BaSO_4$] (highest wave number). These bands are assigned to (M^{2+}–O–H) surface complexation of water with the sulfates. It is further interpreted that the two good-to-perfect cleavages in the mineral group with resultant variation in (M^{2+} - O - H) bond lengths accounts for the existence of the four bands and explain why absorption strength at *ca* 1.91μm (5236cm^{-1}) is not a reliable indication of the overall abundance of water in sulfate minerals. Spectral interpretation within the vicinity of the water combination *ca* 1.91μm (5236cm^{-1}) is further complicated by the presence of a higher wavenumber (v_1 + 4v_3) sulfate combination and the appearance of a band interpreted as the (5v_3) overtone of [SO_4^{2-}]. The results are discussed in the light of these findings.

1. Introduction

The divalent sulfate minerals barite [$BaSO_4$] (alternate spelling baryte), celestine [$SrSO_4$] (alternate spelling celestite) and anglesite [$PbSO_4$] collectively constitute the isostructural (orthorhombic) barite mineral group (C_8 configuration). Alongside other sulfate mineral types these minerals are highly significant in terms of the cycling of metals and sulfate in terrestrial systems [1] and of widespread interest in terms of planetary geology, and with it the search for evidence of water, which is frequently based in large measure on spectroscopic observations and interpretations [2-4].

The molecular sulfate anion [SO_4^{2-}] possesses tetrahedral (T_d) configuration with four mid-infrared absorption features at *ca* 1105cm^{-1} (antisymmetric stretch v_3), 983cm^{-1} (symmetric stretch v_1), 611cm^{-1} (antisymmetric bend v_4) and 450cm^{-1} (symmetric bend v_2) [5,6]. The v_3 and v_4 internal modes are triply degenerate, v_2 is doubly degenerate, v_1 is non degenerate [7]. Barite group minerals are comprised of the strongly bonded structural units ([SO_4^{2-}] tetrahedral) linked by the weaker bonded interstitial metal cations [8]. Generally a molecule has a lower symmetry in a crystal structure because of deformational forces exerted by adjoining extra-molecular interstitial metal cations. In the case of the barite group this lowering of symmetry is expressed through the lifting of triple degeneracy of v_3 and v_4, and double degeneracy of v_2 [6,7].

The mid-infrared spectra of the barite group show linear and nonlinear interstitial cation specific spectral shifts of v_3 and v_1 which are variably ascribed to wavenumber-mass and wavenumber-ionic radius effects, or else dissimilarities in electronic configuration between lead and the periodic group II ions [7]. Interpretation of barite group spectra is complicated by the fact that the isostructural sulfates have a continuous ternary solid solution between barite, celestine and anglesite [9], with compositional intermediates found for all but the anglesite to celestine series in natural environments [9]. Substitution results in changes in unit cell dimensions resulting in spectral changes in wavelength positions of major absorption bands related to changes in S-O bond lengths due to differences in cation size and charge density [10].

Understanding the near–infrared (NIR) spectra of anhydrous sulfates represents a challenge primarily because the highest internal mode vibration of the sulfate ion occurs at *ca* 1100cm^{-1} (9.09μm). This would imply the appearance of at least the fourth overtone of sulfate internal modes. Given that each higher overtone is typically 30 to 100 times weaker than the last [11] it is frequently considered unlikely that many (if any) bands pertaining directly to the sulfate ion will appear in the

NIR, indeed some spectra of barite group powders have been described as spectrally featureless [12]. However, other authors have assigned the 4000 - *ca* 5500cm^{-1} region of NIR spectra to overtone and combination modes of [SO_4^{2-}] internal modes, in addition to any structural or surface adsorbed water which may be present [13].

It is well documented that vibrations of bonds involving hydrogen possess harmonics and combination bands with appreciable absorbance in the NIR, even when minerals are anhydrous and merely possess surface adsorbed water molecules [4]. The strongest NIR absorption for water is the v_2 (antisymmetric stretch) + v_3 (bending vibration) combination band at *ca* 1.9µm (5263cm^{-1}). Bands in the region of *ca* 1.4µm (7140 cm^{-1}) are attributed to the overtones of the fundamental OH stretching modes [14]. Thus a mineral which shows a 1.9µm absorption band contains water and, a mineral which shows a band at 1.4µm but no band at 1.9µm contains only hydroxyl [11]. Therefore the NIR spectra of nominally anhydrous sulfate minerals can be loosely constrained around the basis of surface adsorbed water and/or fluid inclusion based occluded water and/or [OH] vibrations which may potentially occur in combination with water related bending modes [12]. Hence NIR spectra of anhydrous sulfates may potentially yield information on water adsorption and (H_2O) related complexation with sulfates. To this end this study explores aspects of MIR and NIR spectroscopy with reference to synthesised pure end-member compositions of the barite group and a selection of natural barite group mineral spectra.

2. **Materials and methods**

The synthetic [$BaSO_4$] powder was produced by the following method. A solution of $BaCl_2 \cdot 2H_2O$ (3.66g, 0.015mol) in water (100ml) was added dropwise to a solution of sodium sulphate decahydrate (4.48g, 0.014mol) in water (100ml), then the suspension heated at 70^{o}C for 40 minutes. The mixture was allowed to cool, filtered and washed with water. The precipitate was dried at 120^{o}C for 1hour and kept in a desiccator (yield 3.24g). A similar protocol was used for production of [$SrSO_4$], using $SrCl_2 \cdot 6H_2O$ (3.99g, 0.015mol) in water (yield 2.71g), and [$PbSO_4$], using $Pb(NO_3)_2$ (4.96g, 0.015mol). The yield was 4.43g. Natural samples of clear crystalline barite, celestine and anglesite of unknown origin sourced from the University of Brighton geological collection were manually powdered. Samples were measured at room temperature before and after a procedure consisting of oven-drying at 500°C for 168 hours followed by immediate placement in a desiccator and measurement sequentially by NIR and MIR. The NIR analyses were conducted with a Perkin Elmer

Spectrum 100N spectrometer which has a DTGS (deuterated triglycine sulfate) NIR detector. Sample absorbance was measured in the range 4000–10000cm^{-1} using a near-infrared reflectance accessory.

The NIR measurement protocol involved a background scan and a scan type selected to be interleaved (i.e. the shuttle automatically moves to the rear position to take background scan before moving to the front position to scan the sample and display the ratio sample spectrum). The number of scans collected was 8, resolution 16cm^{-1}, optical path difference velocity 1.00 cm/s. The samples were then analysed by MIR. These analyses were performed using a PerkinElmer Spectrum 65 spectrometer, fitted with an attenuated total reflectance (ATR) accessory employing a ZnSe crystal. The samples were measured in the spectral range 550-4000 cm^{-1} at a resolution of 4cm^{-1}. Each spectrum was collected from 16 scans. The MIR Spectrum 65 has a [$LiTaO_3$] (lithium tantalate) detector. Raw data were obtained by the software Spectrum (Perkin Elmer) and further analysed by Peak-Fit (Jandel, Scientific Software). First derivative (Gaussian) peak-fitting procedure was used on all spectroscopic data, with the minimum number of component bands used for the fitting procedure (e.g., [15]). All squared correlations reported are $r^2 > 0.999$. All data was collected at the University of Brighton (United Kingdom) where the synthesised powders and natural samples are stored.

3. The mid infrared (MIR) spectra of the barite group sulfates

The MIR absorption spectra of the natural and synthesised barite-group sulfates are presented in figure 1. The internal mode vibrations are listed in table 1. Within the (900-1300cm^{-1}) region the sharp v_1 bands at 995cm^{-1} [$SrSO_4$], 982cm^{-1} synthetic [$BaSO_4$] and 967cm^{-1} [$PbSO_4$] are in good agreement with previous studies [5-7]. The synthetic barite v_1 band is recorded at 992cm^{-1} and there is a disparity of 6cm^{-1} between the v_4 band position in the natural (632cm^{-1}) and synthetic (638cm^{-1}) barite powders. The reasons for these minor disparities are uncertain, but may stem from the existence of solid solution related impurities within the natural barite sample.

Three v_3 bands are resolved in each spectrum and the respective wavenumbers listed in table 1 apply to the natural and synthetic samples. The weakest of the v_4 bands in each spectrum were resolved by peak-fitting. The v_3 and v_4 data are in good agreement with previous studies (table 1). Of note there is no evidence of mid-infrared absorption around *ca* 3333cm^{-1} (3µm) which would be indicative of the fundamental vibrational modes (v_1, v_3 and $2v_2$) of adsorbed water. Further, there is

no evidence of absorption at *ca* 1645cm^{-1} which would be assignable to (H-O-H) bending. Hence MIR evidence indicates that the three synthetic and three natural powders are at face value anhydrous.

4. The near infrared spectra of the barite group

Figure 2 shows the NIR spectra of the six powders examined. Superimposed on the diagram are H_2O band assignments from [4]. The barite group absorbance highs are broad, generally weak and appear composed of multiple overlapping bands. The strongest band centred at *ca* 5260cm^{-1} (1.9μm) is consistent with combination bend plus stretch absorptions $v_2 + v_3$ (H_2O) at *ca* 1.91μm (5236cm^{-1}) [2]. The subordinate low intensity band at *ca* 1.4μm (7143cm^{-1}) is consistent with overtones of the fundamental OH stretching modes. Hence the six NIR spectra indicate the presence of water. As in the case of the NIR spectrum of anhydrite hosting traces of surface adsorbed water [4] the $v_1 + v_3 + 2v_2$ (H_2O) 1.1μm (9091cm^{-1}) band is not resolved in the synthetic or natural barite group spectra.

For peak-fitting purposes three regions of interest (ROI's) are defined with centres of gravity at *ca* 2.22μm (4500cm^{-1}) (ROI [A]); *ca* 1.9μm (5263cm^{-1}) (ROI [B]); and *ca* 1.4μm (7143cm^{-1}) (ROI [C]). The spectral features enclosed within the three ROI's broadly tally with those previously identified for sulfates of various description [4, 14]. ROI [A] contains six bands which appear common to the natural and synthetic samples. The bands are sequentially labelled [A1] to [A6] with increasing wavenumber relative to the absorption low at *ca* 4260cm^{-1} (Figure 3). ROI [B] contains seven bands which appear common to synthetic and natural spectra. The bands are labelled [B1] to [B7] with increasing wavenumber relative to the absorption low at *ca* 4676cm^{-1} (Figure 4). ROI [C] contains significant background noise which is particularly acute in the spectra of natural [$BaSO_4$] and [$SrSO_4$] in which absorbance is particularly weak. For these reasons peak-fitting of ROI [C] was not practicable. Consequently ROI [C] was not considered for quantitative analysis.

The bands in ROI [A] appear generally sharper in the natural samples, presumably because rapid synthesis of crystals can mean that mineral structures frequently do not re-equilibrate into a well ordered form [16]. Bands [A1] to [A6] from the synthesised powders show wave number variation across the mineral group less than or close to the specified resolution (16cm^{-1}) of the Perkin Elmer Spectrum 100N spectrometer and similar or only marginally greater variability from the natural samples. Therefore correlations between bands within ROI [A] or between bands from ROI [A] with data from ROI [B] are of questionable meaning.

The wave number variation across the mineral group within ROI [B] bands is generally greater than ROI [A] and consistently greater than the specified resolution (16cm^{-1}) of the spectrometer. Of note band [B2] displays a Pearson correlation coefficient of r = 0.9997 at the 95% confidence level between wavenumber and covalent radius of the environment cation for the natural and synthetic powders, plus a series of weaker potential correlations with covalent radius for bands [B1], [B3] and [B4] (Table 2). Data from the seven ROI [B] bands for the natural and synthetic powders are plotted against the covalent radii of the interstitial cation in figure 4. Bands [B1] to [B4] inclusive show positive linear correlations with covalent radius arranged such that [$PbSO_4$] (lowest wave number) → [$SrSO_4$] → [$BaSO_4$] (highest wave number). In all cases the wave number range between [$PbSO_4$] and [$BaSO_4$] is significant with respect to the resolution limit of the spectrometer. Bands [B5], [B6] and [B7] do not show any positive correlations with covalent radii (figure 4). Bands [B1] to [B7] inclusive show no systematic correlation with ionic radius or atomic mass, although it is evident from table 2 that band [B5] data encompasses wave number values consistent with the (H_2O) combination bend plus stretch vibrations at *ca* 1.91µm (5263cm^{-1}).

5. Discussion

The mid-infrared spectra of the synthetic and natural barite group minerals are devoid of spectroscopic evidence for water or hydroxyls. Conversely the near- infrared spectra of ROI's [B] and [C] collectively are wholly compliant with the presence of surface adsorbed water. Given that the MIR and NIR spectra were acquired sequentially it seems highly unlikely that the seeming contradiction between MIR and NIR results stems from laboratory-based sample hydration, not least because the two analytical steps were undertaken sequentially. Instead it is suggested that the absence of MIR evidence for water pertains to the extremely low concentrations of water present in the powders, combined with the fact that higher energy levels exist in NIR spectra because radiation levels from black body emitters peak at shorter wavelengths. Further, the DTGS detector in NIR has a better signal to noise ratio and therefore higher sensitivity than the MIR detector employed in this study. In addition, the strength of absorbance at *ca* 1.95µm (5128cm^{-1}) is not a reliable indicator for estimating (H_2O) abundance because of the dependence of absorbance at these wavelengths on mineral structure [2].

Natural and synthetic samples data from band [B5] most closely encompass the wavenumber interval consistent with the (H_2O) combination bend plus stretch vibration at *ca* 1.91µm (5263cm^{-1})

and are assigned as such. Table 3 and figure 4 indicate the absence of any correlation of band [B5] with covalent radius. Further, plotting [B5] against [B6] and [B7] data also indicate no correlations. As such band [B5] is interpreted to register adsorbed (H_2O) on sample surfaces. Bands [B1] to [B4] inclusive exist as high wavelength shoulders on the (H_2O) combination bend plus stretch vibration and appear systematically correlated to the interstitial cation covalent radii and consequently are interpreted as registering M^{2+} (where M^{2+} = Ba^{2+}, Sr^{2+} or Pb^{2+}) complexation with (H_2O) at surface sites in (M^{2+}−O−H) bend plus stretch assignments.

In the case of natural and synthetic barite (001) and (210) cleavage surfaces are dominant under most experimental conditions [17, 18]. Given that distinct to perfect cleavages on (001) and (210) are also common to celestine and anglesite the same cleavage surfaces may well dominate during spectroscopic analysis of the mineral group as a whole. Specular x-ray reflectivity and atomic force microscopic studies of barite indicate that cleavage surfaces are sites in which near surface sulfate groups exhibit significant structural displacement and water saturation of broken Ba-O bonds [17, 18]. Assuming that the same cleavage surfaces dominate during spectroscopic analysis could well explain the origins of bands [B1] to [B4] inclusive, as barite cleavage surfaces show four distinct Ba-O distances (along the surface normal direction) associated with broken bonds on (001) and (210) surfaces [17, 18]. This interpretation may also account for why absorbance around *ca* 1.95µm (5128cm^{-1}) is not a reliable indicator for estimating H_2O abundance.

Bands in the 4700-4000 cm^{-1} region are commonly assigned to the combinations of the stretching and deformation modes of sulfates (e.g., [14, 19]). NIR band assignments of this region are complicated by the lifting of degeneracy and by the potential existence of solid solution in the natural samples. Nevertheless, a degeneracy-lifted v_3 band (1110cm^{-1} for [$BaSO_4$] and [$PbSO_4$] respectively and 1105cm^{-1} for [$SrSO_4$]) was identified by MIR and has previously been documented [7]. Employing ROI [A] data from the synthetic samples and, assuming that every fundamental will produce a series of absorption bands at (approximately integer) multiples of the internal mode wavenumber the following can be said. The arithmetic multiple ($4v_3$) of this degeneracy-lifted v_3 band is within ≤ 20cm^{-1} of band [A3] data (table 2). Consequently [A3] is assigned as the fourth overtone of this degeneracy-lifted v_3 band.

Comparison of band [A1] data with the ($3v_3$) multiple of the same degeneracy-lifted v_3 band in combination with the v_1 MIR data (listed in table 1) indicates differences of ≤ 31cm^{-1} between the arithmetic sum and band [A1] wavenumber values. Hence, band [A1] could be assigned to a ($3v_3$ + v_1) sulfate combination, as could band [A4] if the combination involved the highest wavenumber

degeneracy lifted v_3 internal mode reported for each mineral in table 1. Similarly, if the lowest wavenumber degeneracy-lifted v_3 bands resolved by MIR are employed in the same combination and a ($4v_3$) assignment the data broadly coincides with the relative positions of the two poorly resolved bands centred around *ca* 4100cm^{-1} and *ca* 4200cm^{-1} respectively (figure 3). Possible origins of the other ROI [A] bands are uncertain. This is because it is not known if the three degeneracy-lifted v_3 bands can occur in combination, or if sulfate internal vibration overtones and combinations can become coupled to external (lattice) modes. Hence, it is possible that much if not all ROI [A] data is related in one way or another to overtones and combinations involving [SO_4^{2-}] internal modes.

Bands [B6] and [B7] are both low in absorbance strength, peripheral to the ($v_2 + v_3$) (H_2O) absorbance high (*ca* 5236cm^{-1}), shows no correlation with M^{2+} covalent radius, or (M^{2+}–O–H) assigned bands and are both poorly resolved, suggesting that the bands may represent a sulfate overtone and or combination band (Fig. 4). With respect to band [B6], employing the ($4v_3$) arithmetic sum of the v_3 bands (1110cm^{-1} for [$BaSO_4$] and [$PbSO_4$] respectively, 1105cm^{-1} for [$SrSO_4$]) in combination with the v_1 data (listed in table 1) the following can be said. It is evident that band [B6] data for the synthetic powders falls within ≤ 7cm^{-1} of the ($v_1 + 4v_3$) arithmetic sum, and is therefore interpreted as a ($v_1 + 4v_3$) sulfate combination band. The origin(s) of band [B7] is less certain although it is of note that the mean of the arithmetic sum ($5v_3$) for the three degeneracy-lifted v_3 bands (table 1) lie within ≤ 55cm^{-1} of all band [B7] data. Accepting that [B7] represents a ($5v_3$) assignment, it follows that the band is either composite in origin (unresolved by peak-fitting) or else, because no polarization dependence can be determined from powders, different vibrations of similar wavenumber appear as a single band [20].

6. Conclusions

Energy levels within the MIR relative to the NIR (in the context of radiation levels from black body emitters), coupled with differences in NIR and MIR analytical detector types, combined with the fact that the detection of water is not simply a function of its abundance but also how it is held to the mineral means that MIR absorbance in isolation is insufficient to detect traces of water. In the case of the nominally anhydrous barite group, it is reasoned that (M^{2+}–O–H) bonding at cleavage surfaces and closely associated with adsorbed (H_2O) potentially carrying bond valence from the interstitial cation to unsatisfied sulfate [SO_4^{2-}] sites provides the best interpretation for the four NIR bands which show a wavenumber correlation with the covalent radius of the interstitial cation. The four bands exist as short wavelength shoulders on the combination bend plus stretch absorption ($v_2 + v_3$)

of (H_2O). In limited experimental conditions the bands could potentially aid mineral identification within the mineral group. Spectral interpretation within the vicinity of the water combination (*ca* 1.91µm (5236cm^{-1}) is complicated by evidence for a sulfate combination and the appearance of a band interpreted as the ($5\nu_3$) overtone of [SO_4^{2-}].

Acknowledgements

The University of Brighton is thanked for financial support. The reviewers are thanked for their comments.

References

[1] I. Chou, R.R. Seal, A. Wang. J. Asian Earth Sci. 63, (2013) 734-758.
http://dx.doi.org/10.1016/j.jseaes.2012.11.027
[2] R.E. Milliken, J.F. Mustard. J. Geophys. Res, 110, (2005) 1-25. doi: 10.1029/2005JE002534,2005.
[3] A. Wang, J.J. Freeman, B.L. Jolliff, I.M. Chou, Geochim. Cosmochim. Acta. 70, (2006) 6118-6135. doi: 10.1016/j.gca.2006.05.022.
[4] Y. Liu (2017) Planet. Space Sci..59 (2018) 1671-1826. https://doi.org/10.1016/jj.pss.2018.04.010.
[5] S.D. Ross. In V. C. Farmer, ed. The infrared spectra of minerals. Min. Soc. Monogr. 18 (1974) 423-444.
[6] M.D. Lane. Am. Mineral. 92 (2007) 1-18.
[7] H.H. Adler, P.F. Kerr. P.F. Am. Mineral. 50 (1965) 132-147.
[8] F.C. Hawthorne. Zeitschrift für Kristallographie. 201 (1992) 183-206.
[9] P.M. Dove, C.A. Czank. Geochchim. Cosmochim. Acta, 59 (1995) 1907-1915.
[10] E.A. Cloutis, F.C. Hawthorne, S.A. Mertzman, K. Krenn, M.A. Craig, D. Marcino, M. Methot, J. Strong, J.F. Mustard, D.L. Blaney, J.F. Bell, F. Vilas. Icarus, 184 (2006) 121-157.
doi: 10.1016/j.icarus.2006.04.003
[11] R.N. Clarke. Spectroscopy of rocks and minerals, and principles of spectroscopy. USGS (1999) http://speclab.cr.usgs.gov
[12] G.R. Hunt, J.W. Salisbury, C.J. Lenhoff. Mod. Geol. (1971) 1-14.
[13] R.L. Frost, R.A. Wills, W. Martens, M. Weier, B.J. Reddy. Spectrochim. Acta A62 (2005) 42-50.
[14] R.L. Frost, B.J. Reddy, E.C. Keeffe. J. Mol. Struct. 977 (2010) 90-99.
doi:10.1016/j.molstruc.2010.05.019
[15] R.L. Frost, A. López, R. Scholz, L. Wang. Spectrochim. Acta A148 (2015) 232-236.

http://dx.doi.org/10.1016/j.ssa.2015.04.011

[16] B.E. Scheetz, W.B. White. Am. Mineral. 62 (1977) 36–50.

[17] P. Fenter, M.T. McBride, G. Srajer, N.C. Sturchio, D. Bosbach. J. Phys. Chem. B105 (2001) 8112-8119.

[18] J.N. Bracco, S.S. Lee, J.E. Stubbs, P.J. Eng, F. Heberling, P. Fenter, A.G. Stack. J. Phys. Chem. C121 (2017) 12236 – 12248. doi:10.1021/acs.jpcc.7b02943

[19] R.L. Frost, D.L. Wain. Spectrochim. Acta A71 (2008) 490-495.

[20] W.B. White. In V.C. Farmer (ed) The infrared spectra of minerals. Mineral. Soc. Monogr. 4, 309 (1974) 227-282.

Captions

Table 1. Mid-infrared (550cm^{-1} to 4000cm^{-1}) wavenumbers internal modes band assignments for synthetic powders. Data in parentheses are comparative values taken from the literature ([a] [7]; [b] [5]; [c] [6]). Reported internal mode band wavenumbers are common to the synthetic (syn) and natural (nat) powders unless otherwise stated.

Table 2. Peak-fitted near-infrared bands for synthesised powders (open brackets) and powdered natural crystals [square brackets]. All data is presented in wavenumbers (cm^{-1}).

Figure 1. Mid-infrared (energy measured by wavenumbers (550-4000cm^{-1})) spectra of the synthetic and natural barite group mineral powders**.**

Figure 2. Near-infrared spectra (energy measured by wavenumbers) of the synthetic and natural barite group mineral powders. Regions of interest (ROI's) [A], [B] and [C] are shown as are water related band assignments (taken from Liu 2017).

Figure 3. Region of interest [A] (energy measured by wavenumbers) near-infrared peak-fitted spectra.

Figure 4. Region of interest [B] (energy measured by wavenumbers) near-infrared peak-fitted spectra.

Figure 5. Region of interest [B] bands, energy measured by wavenumbers (cm^{-1}) plotted against interstitial cation covalent radius picometres (pm). The numbers in brackets are the wavenumber (cm^{-1}) separation between each adjoining member of the barite group. Each ROI [B] band number is

given in brackets followed by a latter to denote whether the data is from a natural (N) or synthetic (S) sample. Where pertinent a r^2 value for the best fit line is given.

Mineral	v_1	v_2	v_3	v_4
[$SrSO_4$] (Celestine)	995	112	1074, 1105, 1176 (1095[a],1081[b], 1179[b])	602, 630,640 (613[b],627[b],642[b])
[$BaSO_4$] (barite)	982 (nat) 992 (syn)	128	1056, 1110, 1184 (1042[b],1114[a],1179[a])	603, 620, 637 (syn) 632 (nat) (611[b],633[b],641[c])
[$PbSO_4$] (anglesite)	967	128	1044, 1110, 1172 (1047[b],1104[a],1164[a])	585, 595, 627 (592[b],597[b],629[b])

341

342 **Table 1**

ROI A Bands	A1	A2	A3	A4	A5	A6	N/A
[$PbSO_4$]	(4314) [4313]	(4369) [4367]	(4450) [4415]	(4482) [4464]	(4541) [4526]	(4601) [4590]	-
[$BaSO_4$]	(4315) [4287]	(4369) [4339]	(4440) [4412]	(4488) [4482]	(4538) [4545]	(4581) [4600]	-
[$SrSO_4$]	(4314) [4309]	(4369) [4360]	(4440) [4427]	(4497) [4489]	(4538) [4535]	(4581) [4589]	-
Wavenumber range (cm^{-1})	(1) [26]	(0) [28]	(10) [15]	(15) [25]	(3) [19]	(20) [11]	-
ROI B bands	**B1**	**B2**	**B3**	**B4**	**B5**	**B6**	**B7**
[$PbSO_4$]	(4802) [4776]	(4947) [4883]	(5091) [5010]	(5202) [5133]	(5281) [5259]	(5414) [5463]	(5598) [5656]
[$BaSO_4$]	(4876) [4802]	(5022) [4980]	(5122) [5105]	(5213) [5194]	(5301) [5278]	(5421) [5423]	(5609) [5611]
[$SrSO_4$]	(4866) [4797]	(5002) [4954]	(5100) [5064]	(5192) [5150]	(5268) [5227]	(5394) [5377]	(5578) [5623]
Wavenumber range (cm^{-1})	(74) [26]	(75) [97]	(31) [95]	(21) [61]	(33) [51]	(27) [46]	(31) [45]
Pearson correlation synthetic	0.9871	0.9997	0.8890	0.3079	0.3962	0.0144	0.1192
Pearson correlation natural	0.9947	0.9997	0.9873	0.8831	0.1390	-0.6604	-0.9997

343

344 **Table 2.**

345

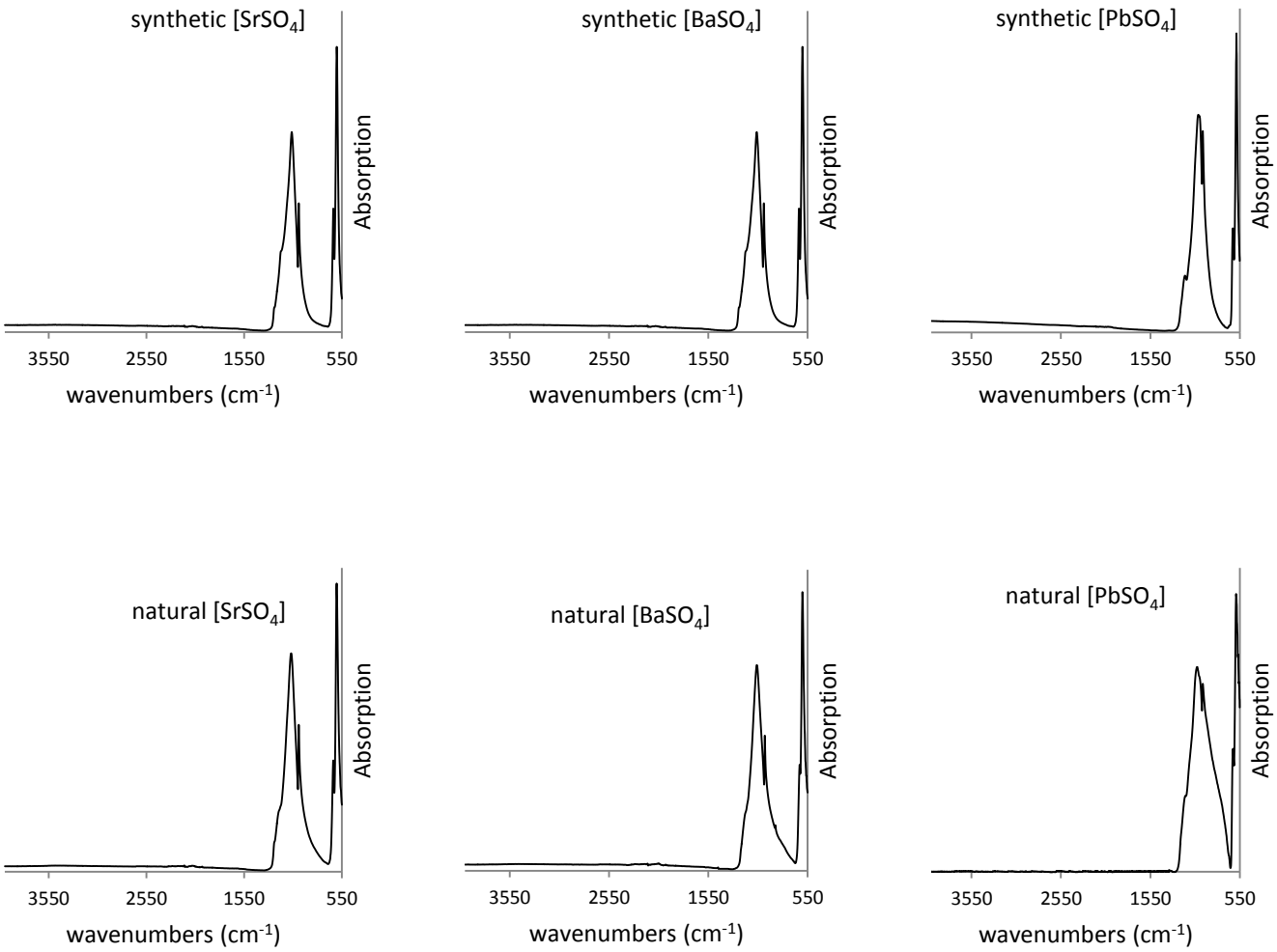
synthetic [SrSO4]
synthetic [BaSO4]
synthetic [PbSO4]
natural [SrSO4]
natural [BaSO4]
natural [PbSO4]
Absorption
3550
2550
1550
550
wavenumbers (cm-1)

Figure 1

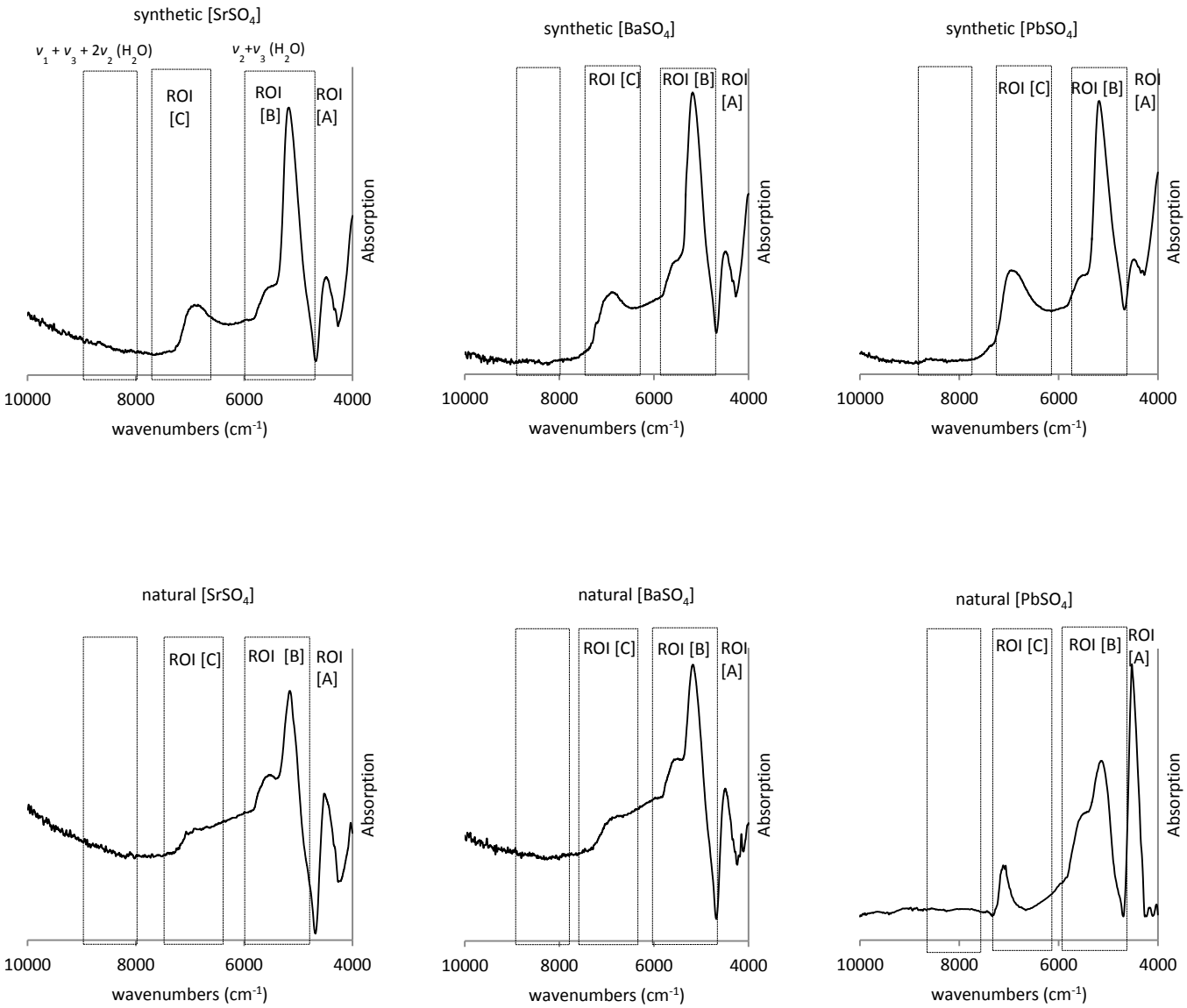
synthetic [SrSO4]
ν1 + ν3 + 2ν2 (H2O)
ν2+ν3 (H2O)
ROI [C]
ROI [B]
ROI [A]
Absorption
10000
8000
6000
4000
wavenumbers (cm-1)
synthetic [BaSO4]
ROI [C]
ROI [B]
ROI [A]
Absorption
10000
8000
6000
4000
wavenumbers (cm-1)
synthetic [PbSO4]
ROI [C]
ROI [B]
ROI [A]
Absorption
10000
8000
6000
4000
wavenumbers (cm-1)
natural [SrSO4]
ROI [C]
ROI [B]
ROI [A]
Absorption
10000
8000
6000
4000
wavenumbers (cm-1)
natural [BaSO4]
ROI [C]
ROI [B]
ROI [A]
Absorption
10000
8000
6000
4000
wavenumbers (cm-1)
natural [PbSO4]
ROI [C]
ROI [B]
ROI [A]
Absorption
10000
8000
6000
4000
wavenumbers (cm-1)

Figure 2

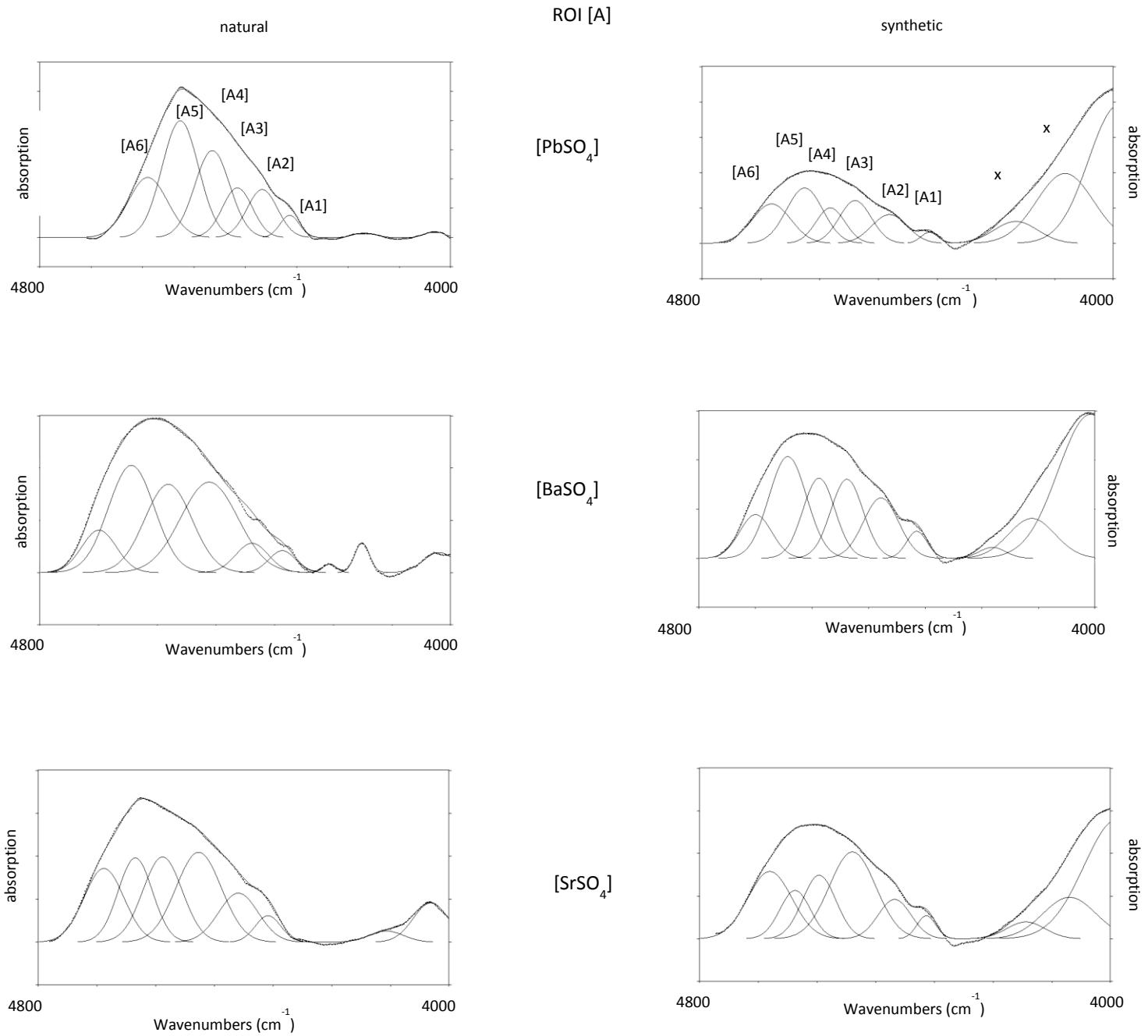
ROI [A]
natural
synthetic
[PbSO4]
[BaSO4]
[SrSO4]
absorption
[A1]
[A2]
[A3]
[A4]
[A5]
[A6]
x
4800
4000
Wavenumbers (cm-1)

Figure 3

natural

ROI [B]

synthetic

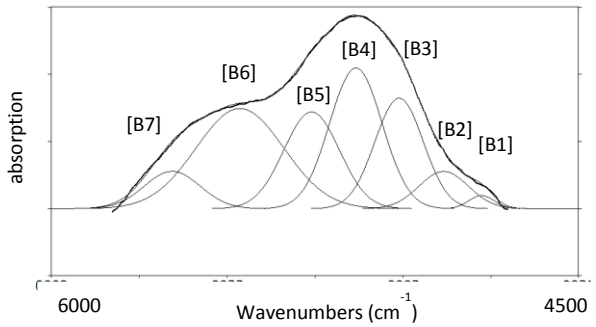

[$PbSO_4$]

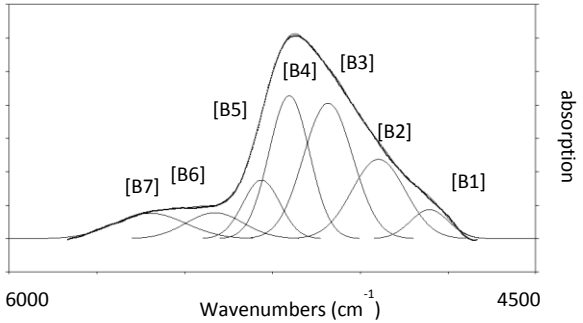

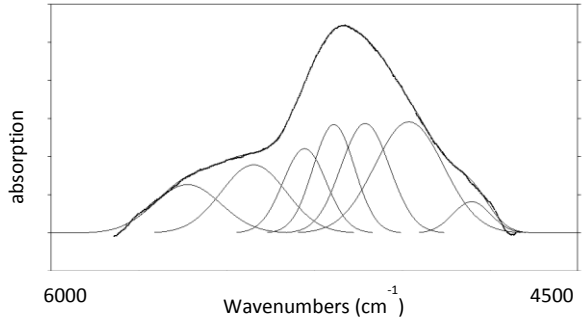

[$BaSO_4$]

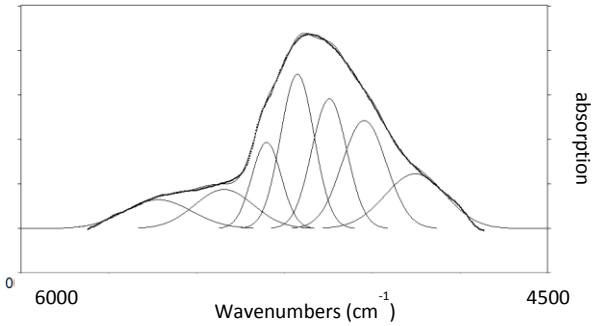

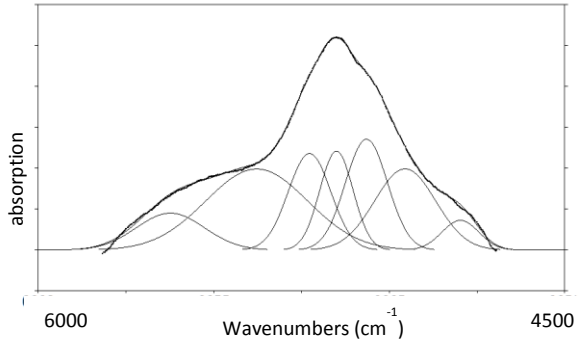

[$SrSO_4$]

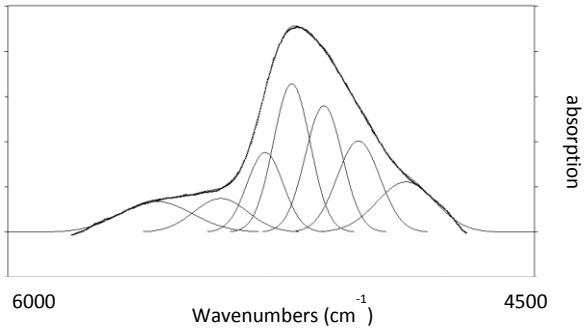

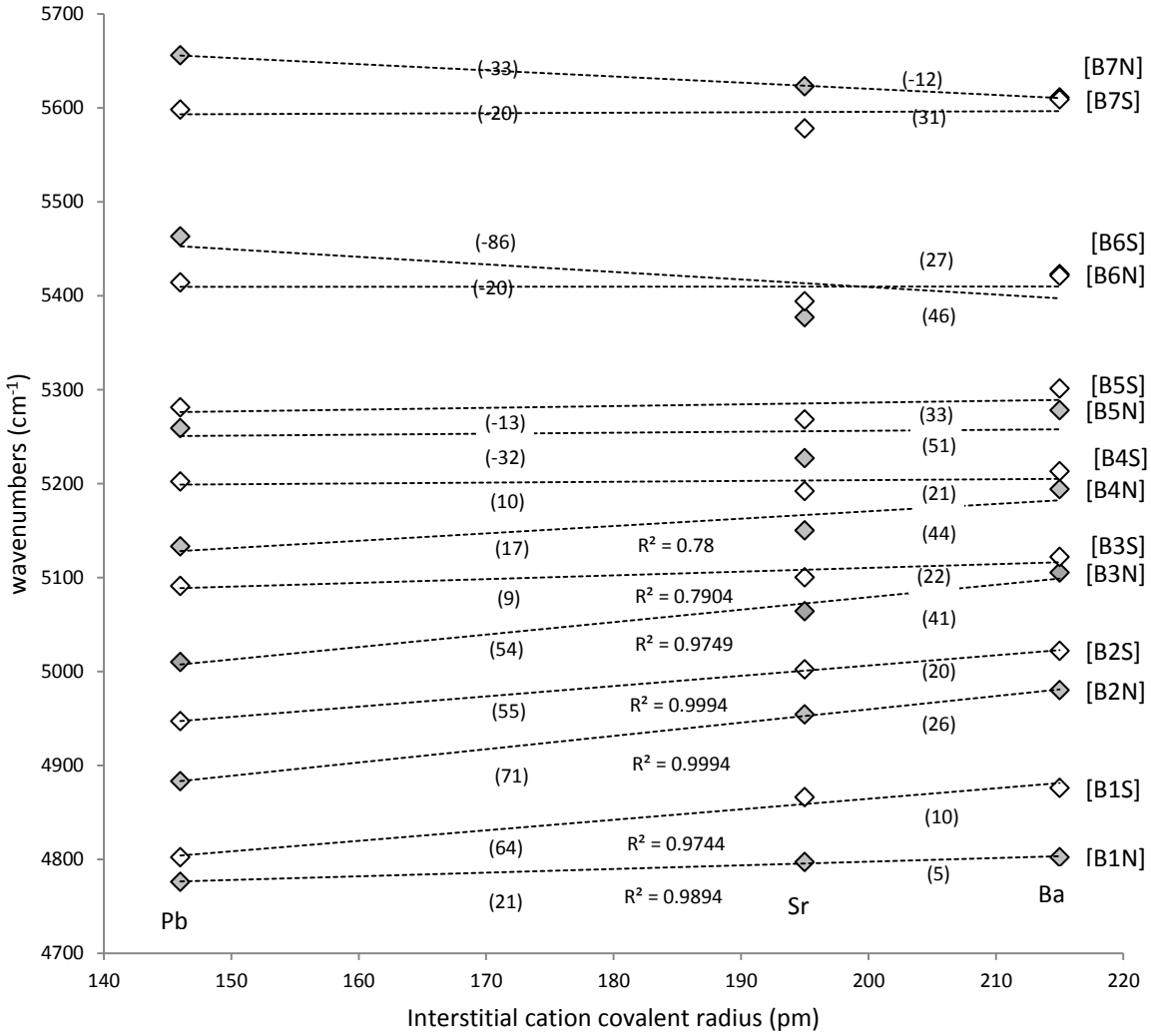
5700
5600
5500
5400
5300
5200
5100
5000
4900
4800
4700
wavenumbers (cm-1)
140
150
160
170
180
190
200
210
220
Interstitial cation covalent radius (pm)
Pb
Sr
Ba
[B7N]
[B7S]
[B6S]
[B6N]
[B5S]
[B5N]
[B4S]
[B4N]
[B3S]
[B3N]
[B2S]
[B2N]
[B1S]
[B1N]
(-33)
(-12)
(-20)
(31)
(-86)
(27)
(-20)
(46)
(-13)
(33)
(51)
(-32)
(10)
(21)
(17)
(44)
(9)
(22)
(54)
(41)
(55)
(20)
(71)
(26)
(64)
(10)
(21)
(5)
R² = 0.78
R² = 0.7904
R² = 0.9749
R² = 0.9994
R² = 0.9994
R² = 0.9744
R² = 0.9894

Figure 5